Applied Acoustics 159 (2020) 107077

Contents lists available at ScienceDirect

Applied Acoustics

journal homepage: www.elsevier.com/locate/apacoust

A methodology for the extrapolation of coast-by noise of tyres from sound power level measurements

Nuria Campillo-Davo *, Ramon Peral-Orts, Hector Campello-Vicente, Emilio Velasco-Sanchez

Miguel Hernandez University of Elche, Avda. de la Universidad, s/n, 03202 Elche, Alicante, Spain

ARTICLE INFO

Article history:
Received 13 February 2019
Received in revised form 3 August 2019
Accepted 29 September 2019
Available online 24 October 2019

Keywords:
Traffic noise
Tyre/road noise
Sound propagation
Model

ABSTRACT

Traffic noise is one of the most predominant noise sources that affect citizens' quality of life in urban areas. The increasing presence of alternative powered vehicles, such as electric or hybrid vehicles, could provide an improvement of such a situation due to the absence of internal combustion engines. However, tyre/road noise is independent of the vehicle type and still exists in alternative powered vehicles. Hence, efforts should focus also on reducing noise emission by means of new tyre designs. The tyre/road noise emission of newly produced tyres is currently evaluated by the Coast-By method, and as a result the rolling sound pressure level at the measuring distance, located 7.5 m away from the test vehicle is obtained. Such an acoustic index provides a very representative data of the annoyance that a pedestrian located at such distance could suffer. However, this value could be affected by external factors, such as environmental conditions. For that reason, this paper presents a methodology for extrapolating the sound pressure levels that are obtained in a Coast-By test, by means of the sound power level emitted by the specific tyre/road combination evaluated. This methodology could serve as the basis for defining a universal model to evaluate a tyre when rolling on a road, by using its sound power emission and predicting the Coast-By sound pressure level.

1. Introduction

Environmental noise is one of the problems that most severely affect citizens in urban areas. Noise pollution is perceived as an annoyance that decreases the quality of life of people exposed to high noise levels, which may have negative consequences, varying from not being able to maintain a conversation to producing sleeping disturbances, alterations in the development of work and other activities that require intense concentration, or variations in the nervous system. Different policies have been developed in the last decades in order to control and reduce environmental noise. In this sense, the "European Commission Green Paper on Future Noise Policy" [1] was a first step towards a common policy on noise in the European Union, identifying traffic noise as the major noise problem in urban and inter-urban environments.

Traffic noise can be considered as the collective contribution of each of the individual vehicles that composes a line of traffic. The noise emitted by a vehicle is produced by different sub-sources [2], which can be grouped into three main categories: noise generated by the power and traction system, noise produced at the tyre/pavement interaction, and aerodynamic noise. Depending on the vehicle speed [3], the sub-sources provide a different contribution: the noise of the power and traction system predominates at low speed, that is, below 30 km/h, whilst at higher speeds the noise coming from the tyre/road interaction prevails. Thanks to new vehicle designs, aerodynamic noise is not currently a relevant source at legal circulation speeds.

The progressive introduction of electric vehicles (EVs) into traffic fleets could represent a reduction of the noise pollution, due to the absence of a mechanical engine in that type of vehicles. However, in [4] it is concluded that the noise emitted by an EV can be compared to the noise emitted by an internal combustion engine (ICE) vehicle without mechanical noise, when they are driving at speeds above 50 km/h. Such a conclusion implies that tyre/road noise is independent of the power supply system, and efforts should focus also on reducing the noise emission of the source, which implies that new silent tyres need to be developed.

The current methodology to evaluate tyre/road noise emission and to obtain the approval of newly produced tyres is known as the Coast-By (CB) method, which is regulated by the UNECE Regulation 117 [5] and based on the ISO 13,325 standard [6]. The assessment methodology is based on measurements at 7.5 m from the test vehicle, which is equipped with the tyres under evaluation, when it passes in front of the measuring point with the engine

* Corresponding author.
E-mail address: ncampillo@umh.es (N. Campillo-Davo).

https://doi.org/10.1016/j.apacoust.2019.107077
0003-682X/

switched off and the transmission in neutral. Although the CB is the current standardized methodology, different authors have pointed out diverse drawbacks of the method [3,7], such as the lack of repeatability due to environmental conditions or background noise, and the fact that it is an expensive method. Besides, the measured magnitude provided by the methodology -the rolling sound pressure level at the measuring distance- could not be the most appropriate to define the rolling noise emission. Other methodologies to evaluate rolling noise can be found in the literature, such as the Close-Proximity method (CPX) [8] or the drum method [9], but they also provide their results as an expression of the sound pressure level.

The acoustic magnitude inherent to a noise source and not dependent on external factors is the sound power level. Very few studies in the literature analyse the sound power level emission of the tyre/road interaction [10–14], and for that reason, the research group authoring this paper developed novel methodologies [15,16,7]. In [15] an Alternative Coast-By (A-CB) methodology was proposed, which provides the rolling sound power level emitted by the whole set of tyres installed on a vehicle. In [16] an Alternative Close-Proximity (A-CPX) test was presented, which provides the sound power level of a single tyre installed on a driven car. In that research, the results of the A-CPX test were used to calculate the tyre/road emission of the whole vehicle, and that value was finally compared with the results of the A-CB test, resulting in an exceptional agreement between both methodologies.

Given the previous background, this paper collects a sound propagation study in which it has been possible to extrapolate the sound pressure level that is obtained in a CB test, using for that purpose the sound power level, previously obtained from an A-CPX test, of the tyre/road combination analysed. The study has been validated by experimental measurements, and a methodology for extrapolating the CB noise of the tested tyre/road combination, by means of its sound power level emission, is finally presented.

2. Materials and methods

The intrinsic property that defines a sound source is its sound power level. This is independent of other external factors like environmental conditions, distance or the orientation of the receiver. Once the sound power level of the source is known, then the sound pressure level at any reception point can be calculated by using a sound propagation model. As mentioned above, the objective of the study is to define a methodology for extrapolating the sound pressure level of the tyre/road noise that would be obtained after measuring the pass-by of a vehicle in CB conditions, by means of using its sound power level emission. Hence, the sound power levels of the tyre/road combination that were evaluated in previous studies are presented in the next sections, as well as the test campaign that was carried out to obtain the experimental CB sound pressure levels at 7.5 m distance of the vehicle. The test environment, in which the test campaign was performed, is also described. Then, an analysis of the application of different sound propagation models is done, in order to calculate the theoretical sound pressure level that is received at the CB reception point. Finally, the results are compared with the experimental sound pressure levels obtained at the CB test campaign, in order to determine a final model for the tyre/road noise tests.

2.1. Sound power level of tyre/road noise

The A-CPX methodology described in [16] allows the assessment of the sound power level that one tyre installed on a vehicle emits when it is running on a road in regular driving conditions. The measurement method is based on the procedures described in the conventional CPX method and also in the ISO 3744 standard [17]. As a result, the tyre rolling sound power level, expressed by the index $L_{W\_A\text{-}CPX}$, is obtained.

The main difference between the A-CPX and the A-CB methodology [15], is that the latter allows the assessment of the sound power level emitted by the tyre/road interaction of the whole set of tyres installed on the vehicle test when it runs on the road test section in CB conditions, that is, with the engine switched off and the transmission in neutral. The A-CB methodology is, in turn, based on the procedures described in the current CB method and in the ISO 3744 standard as well. The result of the test is the sound power level of the whole vehicle's tyre/road noise, expressed by the index $L_{W\_A\text{-}CB}$.

The A-CPX and the A-CB methodologies share the assumption that tyre/road noise is the main vehicle's noise source during the test, and distances between tyres and microphones are enough to consider that far field measurement conditions are fulfilled in both cases. The usual hypothesis of low sound directivity of a rolling tyre in the far field [18] is also assumed. Both methodologies were applied in previous test campaigns to evaluate the noise emission of a set of Pirelli 175/70 R13 82T tyres, installed on a 1991 3-door 1.6 Ford Escort vehicle, when it was driven on dense asphalt. The results obtained were presented as a function of the vehicle speed, following a logarithmic expression, and considering the frequency range from 315 to 4000 Hz. The results were as follows [16]:

$$L_{W\_A-CPX} = 21.0 + 39.9 \cdot \log(v) \quad (\text{dB}) \tag{1.a}$$

$$L_{W\_A-CPX} = 17.0 + 41.9 \cdot \log(v) \quad (\text{dB(A)}) \tag{1.b}$$

$$L_{W\_A-CB} = 27.8 + 40.1 \cdot \log(v) \quad (\text{dB}) \tag{2.a}$$

$$L_{W\_A-CB} = 23.7 + 42.4 \cdot \log(v) \quad (\text{dB(A)}) \tag{2.b}$$

From the previous studies, it was concluded that the sound power level of the rolling noise of the whole vehicle, $L_{W\_TOTAL\_A\text{-}CPX}$, can be calculated from the energetic sum of the sound power level of each individual tyre, Eq. (3). Evaluating that calculation for Eq. (1), Eq. (4) was obtained, which has a strong similarity with Eq. (2) [16].

$$L_{W\_TOTAL\_A-CPX} = 10 \cdot \log_{10}\left(4 \cdot 10^{0.1 \cdot L_{W\_A-CPX}}\right) \quad (\text{dB}) \tag{3}$$

$$L_{W\_TOTAL\_A-CPX} = 27.0 + 39.9 \cdot \log(v) \quad (\text{dB}) \tag{4a}$$

$$L_{W\_TOTAL\_A-CPX} = 23.0 + 41.9 \cdot \log(v) \quad (\text{dB(A)}) \tag{4b}$$

Table 1
$L_{W\_TOTAL\_A\text{-}CPX}$ in one-third octave bands, derived from Eq. (4).

Frequency (Hz)	$L_{W\_TOTAL\_A\text{-}CPX}$ (dB)
200	$L_{W\_TOTAL\_A-CPX@200Hz} = -12.2 + 55.3 \cdot \log(v)$
250	$L_{W\_TOTAL\_A-CPX@250Hz} = 5.8 + 45.2 \cdot \log(v)$
315	$L_{W\_TOTAL\_A-CPX@315Hz} = 22.3 + 34.9 \cdot \log(v)$
400	$L_{W\_TOTAL\_A-CPX@400Hz} = 35.3 + 26.8 \cdot \log(v)$
500	$L_{W\_TOTAL\_A-CPX@500Hz} = 41.6 + 24.2 \cdot \log(v)$
630	$L_{W\_TOTAL\_A-CPX@630Hz} = 16.6 + 39.5 \cdot \log(v)$
800	$L_{W\_TOTAL\_A-CPX@800Hz} = 4.6 + 47.3 \cdot \log(v)$
1000	$L_{W\_TOTAL\_A-CPX@1000Hz} = 7.4 + 46.2 \cdot \log(v)$
1250	$L_{W\_TOTAL\_A-CPX@1250Hz} = 18.1 + 41.0 \cdot \log(v)$
1600	$L_{W\_TOTAL\_A-CPX@1600Hz} = 11.0 + 43.6 \cdot \log(v)$
2000	$L_{W\_TOTAL\_A-CPX@2000Hz} = 6.7 + 45.2 \cdot \log(v)$
2500	$L_{W\_TOTAL\_A-CPX@2500Hz} = 1.5 + 45.9 \cdot \log(v)$
3150	$L_{W\_TOTAL\_A-CPX@3150Hz} = -0.9 + 44.9 \cdot \log(v)$
4000	$L_{W\_TOTAL\_A-CPX@4000Hz} = -1.8 + 43.7 \cdot \log(v)$
5000	$L_{W\_TOTAL\_A-CPX@5000Hz} = -8.7 + 46.1 \cdot \log(v)$

The Eq. (4) has been computed also in the form of one-third octave bands, as shows Table 1. The expressions for the frequency range from 315 to 4000 Hz are collected in the table, as well as the 200, 250 and 5000 Hz one-third octave frequency bands in order to cover the octave bands from 250 to 4000 Hz.

2.2. Tyre/road noise Coast-By measurements

In the present research, experimental measurements have been made according to the CB method, for the same tyre-vehicle-pavement combination used in the previous studies, Fig. 1. During the test campaign, the measuring point was located at 7.5 m away from the vehicle and 1.2 m from the ground. Tests were conducted for six reference speeds: 40, 50, 60, 70, 80 and 90 km/h, and five pass-bys were performed for each speed. Table 2 shows the sound pressure levels registered during the tests, and also includes the average sound pressure level obtained for each reference speed. The results show a stable behaviour of the sound values, and as expected, they show a direct correlation between the speed and the sound pressure level.

2.3. Characterization of the test environment

The test environment in which the test campaigns were carried out influences the sound propagation from the source to the receiver position. Therefore, it was necessary for the present study to acoustically characterize the road test surface. All the tests – those presented in the previous studies as well as those CB tests carried out for the present research – were conducted on the same paved road, composed of a 20 cm thick subbase of graded aggregate, a 20 cm thick base course of graded aggregate, and a surface course consisting of two layers, 5 cm G-20 and 4 cm S-20 with barren porphyry, and sprayed with prime and tack coats, Fig. 2. The tests were carried out on a flat area, with no irregularities on the surface. Given the composition of the pavement, it can be considered to be dense asphalt, of which the acoustic features were characterized by means of the sound absorption coefficient (α) and the Mean Texture Depth (MTD).

The sound absorption coefficient of the road surface was evaluated by means of an impedance tube, according to the guidelines described in the ISO 10844:1994 standard [19], see Fig. 3. Six positions were evaluated, carrying out five measurements in each position, so thirty samples were collected in total. The measurements were made for the frequency range from 400 to 1600 Hz, and the sound absorption coefficient was obtained following the procedure described in the ISO 10844:1994, resulting in a sound absorption coefficient of 0.18 for the test surface. The resulting value can be compared with the results collected in [20], where the absorption coefficient of ordinary asphalt is described. According to those authors, the α value of a conventional pavement increases from values near 0 to 0.2, for the 200 Hz to 800 Hz frequency range, and from the 800 Hz frequency onwards the α values tend to stabilize near 0.2. The absorption coefficient value obtained for the test surface is very close to the value described in the literature, so it can be considered as conventional asphalt.

The Mean Texture Depth analysis was developed according to the procedure described in the EN 13036-1 standard [21], and for that purpose six random positions were selected, and nine measurements were made at each position. The material selected for the test was sand, the composition of which has a granulometry of 100% of the grains with a size greater than 0.2 mm. The granulometry meets the requirement that 90% of the weight of the grains must pass through a sieve of 0.25 mm but not through a 0.18 mm sieve, according to the ISO 565 standard [22]. A volume of 70 ml of sand was spread at each position, with the help of a flat rubber disk, see Fig. 4.

Table 3 collects the MTD test results. The covered average diameter equals to 37.2 cm, which results in a MTD of 0.65 mm. This result agrees with others found in the literature [23] for similar pavements. Moreover, the obtained result meets the requirement of the ISO 10844:1994 for pavements intended for acoustic tests, in which a MTD higher than 0.4 mm is required.

In order to finalize the test road characterization, as can be noticed in Fig. 1, that the test track has a road divider, 4.5 m wide, covered with gravel, which separates the two traffic directions. The road divider must be taken into account when considering the

Fig. 1. Left: Test vehicle and tyres; Right: test environment of the CB measurements.

Table 2
Sound pressure levels registered during the CB test campaign.

Reference speed (km/h)	Sound pressure level (dB(A))					
	Pass-By 1	Pass-By 2	Pass-By 3	Pass-By 4	Pass-By 5	Average
40	60.4	60.2	65.6	63.4	62.0	**62.3**
50	65.1	64.7	65.3	64.6	63.3	**64.6**
60	66.5	67.9	67.9	66.9	68.0	**67.4**
70	69.8	70.6	70.4	70.8	70.3	**70.4**
80	72.3	72.7	72.5	74.0	72.8	**72.9**
90	74.4	74.2	73.3	73.6	73.7	**73.8**

Fig. 2. Detail of the road surface on which tests were conducted.

Fig. 3. Sound absorption coefficient measurements set-up.

sound propagation from the running vehicle to the measurement position, since the measurement position is located 7.5 m away from the vehicle axis and the sound waves encounter the divider on their propagation path. The Fig. 5 shows the geometrical arrangement of the test site, where the measurement position at 7.5 m is located in the test area. The measurement position is located on the southern road direction lane, which is paved with the same dense asphalt than the northern road direction lane where the vehicle test runs during the tests. The measurement position is located at 1.2 m height from the ground.

The gravel which covers the divider has a different sound absorption coefficient from the road surface, usually higher than conventional asphalts. The sound features of different types of gravel have been characterized by some authors [24,25], concluding that the absorption coefficient is comprised between 0.6 and 0.8, depending on the thickness and type of gravel. The gravel that covers the divider is a crushed limestone, for which a sound absorption coefficient of 0.8 and a flow resistivity of 300.5 Ns/m^4 can be considered [26]. These properties will be taken into account when drafting the final model.

2.4. Sound propagation models

The sound propagation from a noise source to a reception location is described in the literature according to different theoretical and empirical models. In all cases, the acoustic pressure $p_{ij}(f)$ generated by a noise source S_i in a reception point M_j, Fig. 6, can be expressed according to Eq. (5) [27]:

$$p_{ij}(f) = A_i(f) \cdot H_{ij}(f) \tag{5}$$

where $A_i(f)$ is the complex amplitude of the source S_i and $H_{ij}(f)$ is the transfer function between reception point and source, which all them depend on the frequency f.

2.4.1. Theoretical modelling of the sound propagation on a flat homogeneous ground

When the sound propagation is produced on a flat homogeneous ground, the transfer function $H_{ij}(f)$ can be expressed according to the model proposed by Rudnick [28], Eq. (6). The model includes both the contribution of the direct path from the source and the receiver and the path of the reflected wave, and also includes the spherical wave reflection factor that in turn depends on the impedance of the ground.

$$H_{ij}(f) = \frac{1}{R_{d,ij}} \cdot e^{J \cdot k_0 \cdot R_{d,ij}} + \frac{Q}{R_{r,ij}} \cdot e^{J \cdot k_0 \cdot R_{r,ij}} \tag{6}$$

where $R_{d,ij}$ is the length of the direct path between source and receiver, $R_{r,ij}$ is the length of the reflected wave path, and using the e^{-Jwt} complex convention where $J^2 = -1$. k_0 is the wave number in the air and Q is the spherical reflection coefficient defined by Eq. (7):

$$Q = R_p + (1 - R_p) \cdot F(w) \tag{7}$$

Being R_p the flat wave reflection coefficient which for a locally reactive soil is expressed according to Eq. (8) [29]:

$$R_p = \frac{(\cos\theta) - \frac{z_0}{z_g}}{(\cos\theta) + \frac{z_0}{z_g}} \tag{8}$$

where z_0 is the characteristic acoustic impedance of the air and z_g is the normal specific impedance of the ground.

The function $F(w)$ describes the interaction of a curved wave front against a surface with infinite impedance. In the case of a flat wave front $F(w)$ tends to 0, while in the case of an infinitely hard surface z_g tends to infinity and hence $F(w)$ tends to 1. For other conditions, the general equation for $F(w)$ is expressed as Eq. (9):

$$F(w) = 1 + 2 \cdot J \cdot w^{1/2} \cdot e^{-w} \cdot \int_{-J \cdot w^{1/2}}^{\infty} e^{-u^2} \cdot du \tag{9}$$

Being w the numerical distance, Eq. (10):

$$w = \frac{1}{2} \cdot J \cdot k_0 \cdot R_{r,ij} \cdot \left[(\cos\theta) + \frac{z_0}{z_g} \right]^2 \tag{10}$$

The ground impedance can be expressed by any impedance model that fits the properties of the ground under study. The model proposed in [30] and updated by [31], equation (11), is suitable in the case of surfaces covered by porous and fibrous materials [32], as grass or vegetation. In the model a local sound reaction is considered and the only parameter that is taken into account is the specific flow resistivity, σ, expressed in Nsm^{-4}.

$$\frac{z_g}{z_0} = 1 + 5.5 \cdot \left(\frac{f}{\sigma}\right)^{-0.632} + J \cdot 8.43 \cdot \left(\frac{f}{\sigma}\right)^{-0.632} \tag{11}$$

For porous surfaces, as absorbing asphalts, the hypothesis of a local reaction is not valid, due to the need to consider the angle of incidence of the sound waves that affect the surface. Hence, in that case the acoustic impedance is defined according to the model

Fig. 4. Sand sample used for the MTD tests, test procedure and measurement point.

Table 3
Mean texture depth test results.

MTD TEST RESULTS (cm)								
Measurement number	Measurement position							
	1	2	3	4	5	6		
1	36	36	38	37	37.5	39.5		
2	37	35	38	36.5	38	39		
3	35	34.5	39	37.5	38	38.5		
4	36	35	37.5	38	38.5	39		
5	35.5	36	37	38	39	39		
6	35.7	35	37	37.5	39	39		
7	36.5	35	37.5	37	37.5	39		
8	36.5	35	37.5	36.5	37	38.5		
9	36	36	37.5	37	38	39		
Average (cm)	**36.02**	**35.28**	**37.67**	**37.22**	**38.06**	**38.94**	**Global average (cm)**	**37.2**
MTD (mm)	**0.69**	**0.72**	**0.63**	**0.64**	**0.62**	**0.58**	**MTD average mm)**	**0.65**

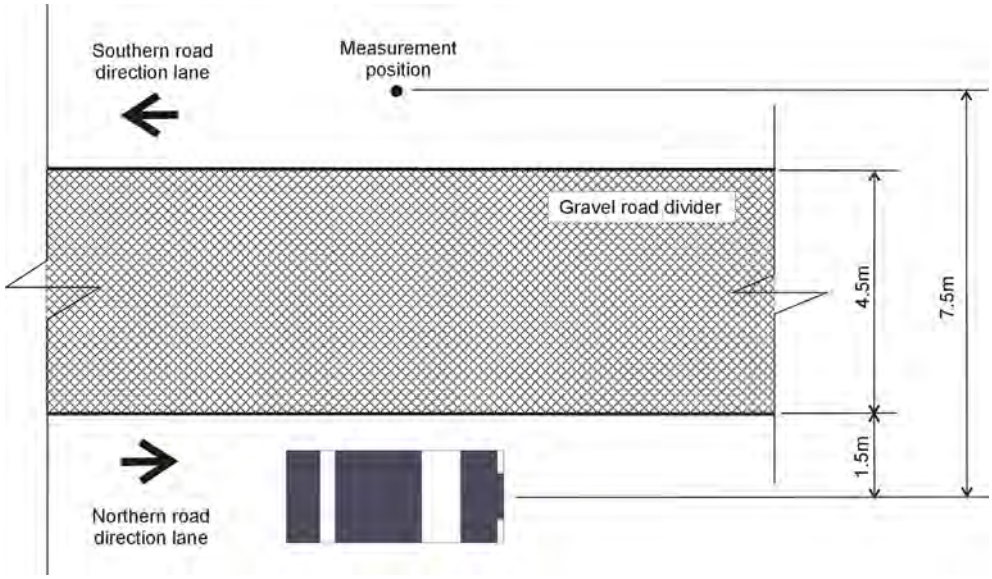

Fig. 5. Geometric arrangement of the test site.

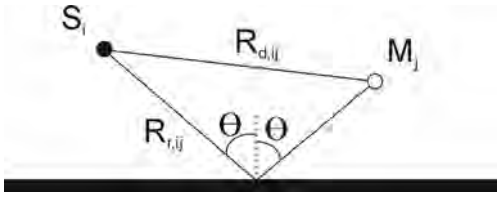

Fig. 6. Geometrical conditions of sound propagation, extracted from [27].

described in [33], Eq. (12), in which three parameters are used: the porosity (expressed in %), the specific flow resistivity σ(expressed in kNs/m^4) and the form factor or tortuosity K.

$$z_g = \rho_0 \cdot c_0 \cdot \frac{1}{\Omega} \cdot \sqrt{\frac{K}{\gamma}} \cdot \frac{\sqrt{1 - J \cdot \frac{f_u}{f}}}{\sqrt{1 - \left(1 - \frac{1}{\gamma}\right) \cdot \frac{1}{1 - J\frac{f_\vartheta}{f}}}} \tag{12}$$

where $\gamma = c_p/c_v = 1.4$ is the ratio of the specific heat for air; and $f_u = \frac{\sigma \cdot \Omega}{2\pi \cdot \rho_0 \cdot K}$ and $f_\vartheta = \frac{\sigma}{2\pi \cdot \rho_0 \cdot N_{pr}}$ are the characteristic frequencies associ-

ated with thermal and viscous effects respectively, being $N_{pr} = 0.71$ the dimensionless number of Prandtl for air.

In the case of totally reflecting surfaces, as non-porous asphalts, the boundary condition is infinite acoustic impedance.

2.4.2. Theoretical modelling of the sound propagation on a discontinuous impedance ground

When the sound propagation is not produced on a flat and homogeneous ground, but is produced on a ground with discontinuous impedance, that is, with changes in the ground material, the transfer function $H_{ij}(f)$ that describes the sound propagation must include those changes. The model proposed by Rasmussen [34] takes this into account, Eq. (13), including different spherical wave reflection factors for each ground type.

$$H_{ij}(f) = \frac{\sqrt{8\pi \cdot k_0} \cdot d_{disc,j} \cdot e^{J\cdot\frac{\pi}{4}}}{\sqrt{16\pi^2}} \cdot \int_0^{\infty} G_{ij}(z)dz \tag{13}$$

Being $d_{disc,j}$ the distance between the impedance change and the measurement position, and where:

$$\begin{aligned} G_{ij}(z) = & \frac{e^{J\cdot k_0\cdot(R_{1,ij}+R_{3,ij})}}{\sqrt{R_{3,ij}^3 \cdot R_{1,ij} \cdot (R_{1,ij}+R_{3,ij})}} \\ & + Q_{2,ij} \cdot \frac{e^{J\cdot k_0\cdot(R_{1,ij}+R_{4,ij})}}{\sqrt{R_{4,ij}^3 \cdot R_{1,ij} \cdot (R_{1,ij}+R_{4,ij})}} \\ & + Q_{1,ij} \cdot \frac{e^{J\cdot k_0\cdot(R_{2,ij}+R_{3,ij})}}{\sqrt{R_{3,ij}^3 \cdot R_{2,ij} \cdot (R_{2,ij}+R_{3,ij})}} \\ & + Q_{1,ij} \cdot Q_{2,ij} \cdot \frac{e^{J\cdot k_0\cdot(R_{2,ij}+R_{4,ij})}}{\sqrt{R_{4,ij}^3 \cdot R_{2,ij} \cdot (R_{2,ij}+R_{4,ij})}} \end{aligned} \tag{14}$$

Being $Q_{1,ij}$ and $Q_{2,ij}$ the spherical reflection coefficient when taking into account the direct and reflected waves over ground 1 and 2 respectively, between sound source and receiver point and a point located on the vertical of the discontinuity, see Fig. 7. Those coefficients have the same form as expressed in Eq. (7).

2.4.3. Empirical model of the sound propagation

The models presented in the previous sections provide a theoretical calculation scheme for contemplating the effects of surfaces with finite and infinite impedance as well as the effects caused by discontinuities in the medium. However, empirical models are usually employed in the engineering field and in that sense, the model proposed by the ISO 9613-2 standard [35], is commonly used due to its simplicity and ease of implementation, especially for experimental studies [36]. It consists of an engineering method whose formulation is based on algorithms in octave bands in the frequency range from 63 Hz to 8 kHz. It takes into consideration

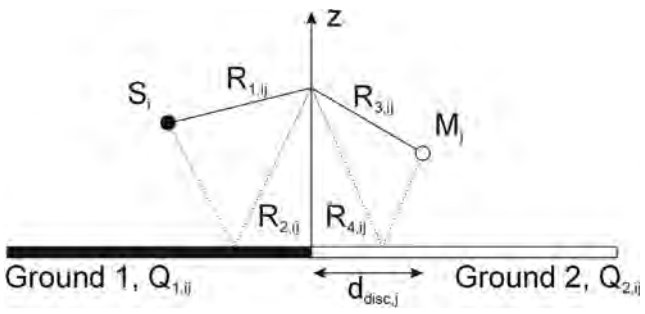

Fig. 7. Geometrical conditions of sound propagation on a discontinuous impedance ground, extracted from [27].

the effects on the sound propagation due to the geometrical divergence, the atmospheric absorption, the effect of ground characteristics, the reflexions generated by other nearby surfaces and the screening effects generated by other objects. The basic expression of the method, Eq. (15), relates the equivalent continuous sound pressure level in octave bands, $L_{fT}(DW)$, as a function of the sound power level L_W emitted by the point sound source, the directivity correction D_I, and the attenuation factor A.

$$L_{fT}(DW) = L_W + D_I - A \quad (\text{dB}) \tag{15}$$

At the same time, the attenuation factor depends on different features, as described in Eq. (16).

$$A = A_{div} + A_{atm} + A_{gr} + A_{bar} + A_{misc} \tag{16}$$

where A_{div} is the geometric divergence, which also depends on the distance d between source and receiver, according to Eq. (17).

$$A_{div} = 20 \cdot \log(d) + 11 \tag{17}$$

A_{atm} is the atmospheric absorption attenuation, which is a function of the distance d and the atmospheric attenuation coefficient α, in dB/km, in octave bands, Eq. (18).

$$A_{atm} = \alpha \cdot d/1000 \tag{18}$$

The attenuation due to ground effect A_{gr}, Eq. (19), depends on the attenuation factor of the source region A_s characterized by the ground factor of the cited region G_s, on the attenuation factor of the receiver region A_r characterized by the ground factor of such region G_r, and on the attenuation factor of the middle region characterized by its ground factor G_m.

$$A_{gr} = A_s + A_r + A_m \tag{19}$$

The source region covers the distance from the source (located at an h_s height) to the receiver (located at an h_r height) included within the value $30{\cdot}h_s$, till a maximum of d_p, which is the distance projected on the ground between source and receiver. The receiver region comprises the distance from the source to the receiver included within the value $30{\cdot}h_r$, again till a maximum of d_p. Finally, the middle region is the distance between source and receiver regions. There is no middle region when the expression $d_p < (30{\cdot}h_s + 30{\cdot}h_r)$ is fulfilled.

Regarding the ground factor G for each region, three cases are considered: hard ground, $G = 0$, which includes paved surfaces, water, ice, concrete and other surfaces with low porosity; porous ground, $G = 1$, which includes grass, trees and vegetation; and mixed ground, for which $0 < G < 1$. The different attenuation factors G (where $G = G_s$ when referring to source region calculations and $G = G_r$ when referring to receiver region calculations) are described with more detail in the Table 3 of the ISO 9613-2 standard.

The attenuation due to barriers, A_{bar}, is applied when the density of an object located between source and receiver is at least 10 kg/m^2; it has a closed surface; and its horizontal dimension perpendicular to the source-receiver line is larger than a wavelength of the nominal frequency for the octave band of interest.

Finally, the attenuation due to some other effects, A_{misc}, includes the attenuation due to the propagation through foliage, industrial sites or urbanized areas.

3. Results and discussion

The results of calculation of sound pressure levels derived from the sound power levels, by means of the propagation models described before, are presented in this section, Tables 4–6. The calculations have been done using the sound power levels described in Table 1, and hence the results are expressed in one-third octave bands. Also the overall value results obtained from the overall

Table 4
Sound pressure levels according to Rudnick's model, for a homogeneous reflecting ground.

$L_{pi\_Rudnick}$ (dB(A))						
Frequency (Hz)	Reference speed (km/h)					
	40	50	60	70	80	90
315	46.7	50.0	52.8	55.4	57.6	59.1
400	49.0	51.6	53.8	55.7	57.5	58.6
500	53.0	55.2	57.2	59.0	60.6	61.6
630	52.7	56.5	59.7	62.6	65.2	66.8
800	53.8	58.3	62.2	65.6	68.7	70.6
1000	55.7	60.1	63.9	67.3	70.2	72.2
1250	59.0	62.9	66.3	69.3	71.9	73.6
1600	56.3	60.4	64.0	67.2	70.0	71.8
2000	54.7	58.9	62.7	66.0	68.9	70.8
2500	50.7	55.0	58.8	62.1	65.1	67.0
3150	46.6	50.9	54.6	57.9	60.7	62.6
4000	43.7	47.8	51.4	54.6	57.4	59.2
Overall value	**64.7**	**68.7**	**72.1**	**75.2**	**77.9**	**79.6**

Table 5
Sound pressure levels according to Rasmussen's model, for a ground with impedance change.

$L_{pi\_Rasmussen}$ (dB(A))						
Frequency (Hz)	Reference speed (km/h)					
	40	50	60	70	80	90
315	47.1	50.4	53.2	55.8	58.0	59.5
400	49.4	52.0	54.2	56.1	57.9	59.0
500	53.4	55.6	57.6	59.4	61.0	62.0
630	52.9	56.7	59.9	62.8	65.4	67.0
800	53.3	57.8	61.7	65.1	68.2	70.1
1000	51.7	56.1	59.9	63.3	66.2	68.2
1250	51.0	54.9	58.3	61.3	63.9	65.6
1600	48.3	52.4	56.0	59.2	62.0	63.8
2000	50.8	55.0	58.8	62.1	65.0	66.9
2500	48.6	52.9	56.7	60.0	63.0	64.9
3150	44.1	48.4	52.1	55.4	58.2	60.1
4000	38.9	43.0	46.6	49.8	52.6	54.4
Overall value	**60.7**	**64.7**	**68.1**	**71.2**	**73.9**	**75.6**

Table 6
Sound pressure levels according to ISO 9613–2 model, for a ground with impedance change.

$L_{pi\_ISO\text{-}9613\text{-}2}$ (dB(A))						
Frequency (Hz)	Reference speed (km/h)					
	40	50	60	70	80	90
250	45.8	49.9	53.6	56.9	59.9	61.9
500	53.4	56.2	58.8	61.1	63.2	64.6
1000	59.2	63.4	67.0	70.2	73.1	74.9
2000	57.7	61.9	65.6	68.9	71.7	73.6
4000	47.2	51.4	55.0	58.3	61.2	63.1
Overall value	**61.5**	**65.5**	**68.9**	**72.0**	**74.7**	**76.4**

Eq. (4) are presented in the last row of Tables 4–6. The results of the ISO 9613-2 calculations are presented in octave bands, instead of one-third octave bands, according to the standard prescriptions. For the calculations, the equivalent sound source has been considered to be located on the ground, 0 m height, at the geometric centre of the vehicle.

The first calculation under study considers a flat homogeneous ground surface between source and receiver. Given that the asphalt surface of the test site has a very low absorption coefficient, the hypothesis of reflecting material is taken. In such a case, the Rudnick's propagation model is used by means of the ground attenuation considered in [37]. Then, the sound pressure level at a reception point located at a distance d is expressed by the Eq. (20). The Table 4 collects the sound pressure levels obtained.

$$L_{pi\_Rudnick} = L_{W\_TOTAL\_A-CPX} - 10 \cdot \log_{10}\left(4\pi \cdot d^2\right) + Att_{gr\_Rudnick} \quad (\text{dB}) \tag{20}$$

The second case under study considers the impedance change produced by the road divider. Given the proximity of the vehicle to the road divider, the geometrical configuration of the test site, Fig. 5, can be initially approximated to the configuration studied in [37] according to Rasmussen's model. In such a study, a porous surface followed by a reflecting surface where the receiver is located was modelled, and the sound attenuation relative to free field was obtained. The sound pressure levels at the reception point are collected in Table 5, evaluated by the implementation of equation (21). The data for the overall expression have been calculated by using the attenuation terms for 1000 Hz.

$$L_{pi\_Rasmussen} = L_{W\_TOTAL\_A-CPX} - 10 \cdot \log_{10}\left(4\pi \cdot d^2\right) + Att_{gr\_Rasmussen\ i} \quad (\mathrm{dB}) \tag{21}$$

The propagation model proposed in the ISO 9613-2 considers the atmospheric attenuation factor in addition to ground and distance attenuations, contemplated also in the other two models. The attenuation due to barriers and the attenuation due to other effects do not apply to the test conditions in the present research. The Table 6 collects the sound pressure levels calculated at the reception point, are evaluated by the implementation of Eq. (22). In this case, the *G* factors assigned to the asphalt surface and the gravel divider are 0.18 and 0.8, respectively, and the attenuation due to atmospheric absorption has been calculated for environmental conditions of 25 °C and 30%HR [38]. According to the standard guidelines, the results for the overall value have been obtained by using the attenuation terms for 500 Hz.

$$L_{pi\_ISO-9613} = L_{W\_TOTAL\_A-CPX} + D_C - A_{div} - A_{atm} - A_{gr} \quad (\mathrm{dB}) \tag{22}$$

The results presented in the previous tables show an increment of sound pressure levels with speed in all cases, while the central frequency bands present the higher levels. The results for Rudnick's model provide higher levels at the reception point than Rasmussen's and ISO 9613-2 models, for the overall values. The Table 7 summarizes the overall theoretical values and experimental results of the CB test campaign, and provides a comparison of the differences in absolute values between the theoretical and experimental results.

The results show that the minimum differences between the theoretical and the experimental values are obtained for those models which take into account the impedance change in the ground, that is Rasmussen's and ISO 9613-2 models. Generally speaking, the Rasmussen's model presents the best behaviour for all reference speeds, showing a maximum deviation of 1.8 dB for the highest speed. The model proposed according to the guidelines of the ISO 9613-2 shows higher deviation than the Rasmussen's model in comparison with the experimental results. However, the standard estimates that the method has an accuracy of ±3 dB, which is met in all cases. Regarding the Rudnick's model, the deviation from the experimental results is higher than for the other models, presenting an average deviation of 4.5 dB.

The Rasmussen's model is a complex sound propagation model, which requires a high computational cost for its implementation as well as advanced acoustic knowledge. The Rudnick's model is also a complex model; however, it presents a high deviation from the experimental results, mainly due to the absence of impedance change in the model, which does not fit with the test environment. On the other hand, the model collected in the ISO 9613-2 standard is much simpler to implement than the others, its use is very widespread, it presents an adequate uncertainty for the sound source being evaluated in the present research, and it allows the sound pressure level to be directly evaluated in an overall value instead of by frequency bands.

Given all the aspects mentioned above, the propagation model of the ISO 9613-2 has been applied to pose the relation between the power emission and the sound pressure levels under the test conditions described in the present research. In that sense, the Eq. (23), can be used to extrapolate the sound pressure level that will be received at 7.5 m, $L_{p\_7.5m}$, from the test vehicle when it is driven in CB conditions on the test site described in the previous sections, that is, when its noise emission mainly comes from the tyre/road interaction, and once the sound power level emission of one of its tyres is known, $L_{W\_A\text{-}CPX}$.

$$L_{p\_7.5m} = L_{W\_A-CPX} - 19.9 \quad (\mathrm{dB(A)}) \tag{23}$$

By adopting the same methodology that has been used to obtain Eq. (23), the behavior of different combinations of tyre/road could be modeled, allowing obtaining a general model in further studies.

4. Conclusions

The current methodology for the approval of newly produced tyres, the Coast-By (CB) method, has been discussed to present some drawbacks that make it question its applicability for assessing tyre/road noise. The result that provides such method, the sound pressure level at 7.5 m from the tested vehicle, is a very representative data of the annoyance that a pedestrian located at such distance could suffer. However, the method does not provide an effective value of the rolling tyre sound emission. The intrinsic property that characterizes a noise source is its sound power emission, and for that reason, it seems more convenient to evaluate the emission of a rolling tyre by means of its sound power level. Once the sound power level is known, then the sound pressure level at any reception point can be calculated.

The work presented in this paper is the continuation of an extensive study dedicated to the analysis and characterization of the sound emitted during the tyre/road interaction, in which two different alternative methodologies (A-CB and A-CPX) were previously designed to evaluate the sound emission of the source by means of its sound power level. In this paper, a study of the extrapolation of the sound pressure level that would be received at 7.5 m distance, due to the passing of a vehicle whose only noise source comes from the tyre/road interaction, and on a specific tyre/road combination, has been presented. The extrapolation methodology requires that the sound power emission of one of its tyres is previously known. The attenuation effects due to the sound propagation from the emitter to the receiver are included in the resulting extrapolation equation. Thereby, the proposed methodology could be used as an alternative procedure to the current Coast-By method. The extrapolation presented in this paper has been developed for a tyre/road combination only, being useful as a validation of the methodology proposed. For future work, new tyre/road combinations installed on different vehicle types will be tested with the aim to obtain a universal extrapolation model.

Table 7
Comparison of theoretical and experimental results.

Reference speed (km/h)	40	50	60	70	80	90	
Theoretical and Experimental results (dB(A))							
$L_{p\_Rudnick}$	64.7	68.7	72.1	75.2	77.9	79.6	
$L_{p\_Rasmussen}$	60.7	64.7	68.1	71.2	73.9	75.6	
$L_{p\_ISO\text{-}9613\text{-}2}$	61.5	65.5	68.9	72.0	74.7	76.4	
$L_{p\_Experimental\ CB}$	62.3	64.6	67.4	70.4	72.9	73.8	
Difference theoretical models – experimental measurements (dB)							**Average**
$\lvert L_{p\_Rudnick} - L_{p\_Experimental\ CB}\rvert$	2.4	4.1	4.7	4.8	5.0	5.8	**4.5**
$\lvert L_{p\_Rasmussen} - L_{p\_Experimental\ CB}\rvert$	1.6	0.1	0.7	0.8	1.0	1.8	**1.0**
$\lvert L_{p\_ISO\ 9613\text{-}2} - L_{p\_Experimental\ CB}\rvert$	0.8	0.9	1.5	1.6	1.8	2.6	**1.3**

Acknowledgements

The work in this paper was partially funded within the framework of the Projects of Scientific Research and Technological Development Bancaja – UMH (RR1522/09).

References

[1] Commission Green Paper, on Future Noise Policy. 4 November 1996.
[2] Nelson P. Transportation Noise Reference Book. Butterworths-Heinemann; 1987.
[3] Sandberg U, Ejsmont JA. Tyre/road noise reference book. Kisa, Sweden: Informex; 2002.
[4] Campello-Vicente H, Peral-Orts R, Campillo-Davo N, Velasco-Sanchez E. The effect of electric vehicles on urban noise maps. Appl Acoust 2017;116:59–64.
[5] UNECE Regulation 117. Uniform provisions concerning the approval of tyres with regard to rolling sound emissions and to adhesion on wet surfaces 2007.
[6] International Organisation for Standardization. ISO 13325:2003. Tyres – Coast-by methods for measurement of tyre-to-road sound emission.
[7] Clar-Garcia D, Velasco-Sanchez E, Campillo-Davo N, Campello-Vicente H, Sanchez-Lozano M. A new methodology to assess sound power level of tyre/road noise under laboratory controlled conditions in drum test facilities. Appl Acoust 2016;110:23–32.
[8] International Organisation for Standardization. ISO 11819-2:2017. Acoustics – Measurement of the influence of road surfaces on traffic noise – Part 2: The close-proximity method.
[9] Sandberg U. Possibilities to replace outdoor coast-by tyre/road noise measurements with laboratory drum measurements. Swedish Road and Transport Research Institute (VTI), Silence Consortium; 2005.
[10] Meiarashi S, Ishida M. Noise reduction characteristics of porous elastic road surfaces. Appl Acoust 1996;47(3):239–50.
[11] Yoshihisa K, Tachibana H. Sound power level measurements for road vehicles by using the square-integrating technique. Proceedings of INTERNOISE 88.
[12] Cho DS, Mun S. Determination of the sound power levels emitted by various vehicles using a novel testing method. Appl Acoust 2008;69(3):185–95.
[13] Peeters B, van Blokland G. The noise emission model for European road traffic. Deliverable 11 of the IMAGINE project, IMA55TR-060821-MP10. January 11th. 2007.
[14] Tsukui K, Oshino Y, van Blokland G, Tachibana H. Study of the road traffic noise prediction method applicable to low-noise road surfaces. Acoust Sci Technol 2010;31:102–12.
[15] Campillo-Davo N, Peral-Orts R, Velasco-Sanchez E, Campello-Vicente H. An experimental procedure to obtain sound power level of tyre/road noise under Coast-By conditions. Appl Acoust 2013;74:718–27.
[16] Campillo-Davo N, Peral-Orts R, Campello-Vicente H, Velasco-Sanchez E. An alternative close-proximity test to evaluate sound power level emitted by a rolling tyre. Appl Acoust 2019;143:7–18.
[17] International Organisation for Standardization. ISO 3744:2010. Acoustics – Determination of sound power levels and sound energy levels of noise sources using sound pressure – Engineering methods for an essentially free field over a reflecting plane.
[18] Ibarra Zárate DI. Contribution of the noise radiated by a single vehicle to the road traffic noise Doctoral Thesis. Universidad Politecnica de Madrid; 2013.
[19] International Organisation for Standardization. ISO 10844:1994. Acoustics – Specification of test tracks for the purpose of measuring noise emitted by road vehicles.
[20] Wang L, Xing Y, Chang C. The noise-reducing character of OGFC pavement with crumb rubber modified asphalt. Proc Int Conf Trans Eng 2009;3:1820–5.
[21] CEN Comité European de Normalization. EN 13036-1:2010. Road and airfield surface characteristics. Test methods. Part 1: Measurement of pavement surface macrotexture depth using a volumetric patch technique.
[22] International Organisation for Standardization. ISO 565:1990. Test sieves – Metal wire cloth, perforated metal plate and electroformed sheet – Nominal sizes of openings.
[23] Hanson DI, Prowell BD. Evaluation of circular texture meter for measuring surface texture of pavements NCAT Report 04-05. National Center for Asphalt Technology; 2004.
[24] Egan MD. Architectural acoustics. J. Ross Publishing; 2007.
[25] Heggies Pty Ltd. Gladstone LNG Facility Noise Assessment. REPORT 20-2014-R7. Revision 3. 2010.
[26] Rossi TJ. Behavior of low-frequency sound waves in porous media Doctoral Thesis. University of Illinois; 2010.
[27] Golay F, Dutilleux G, Ecotière D. Source height determination for several sources at the same height. Acta Acustica United Acustica 2010;96:863–72.
[28] Rudnick I. The propagation of an acoustic wave along a boundary. J Acoust Soc Am 1947;143:348–57.
[29] Embleton TFW, Piercy JE, Olson N. Outdoor sound propagation over ground of finite impedance. J Acoust Soc Am 1976;59:267–77.
[30] Delany ME, Bazley EN. Acoustical properties of fibrous absorbent materials. Appl Acoust 1970;3:105–16.
[31] Miki Y. Acoustical properties of fibrous absorbent materials. Modifications of Delany-Bazley models. J Acoust Soc Japan 1990;11:19–24.
[32] Juliá Sanchis E. Modelización, simulación y caracterización acústica de materiales para su uso en acústica arquitectónica Doctoral Thesis. Politechnic University of Valencia; 2008.
[33] Hamet JF, Bérengier M. Acoustical characteristics of porous pavements: a new phenomenological model. Proceedings of INTER-NOISE 93. Leuven, Belgium.
[34] Rasmussen KB. A note on the calculation of sound propagation over impedance jumps and screens. J Sound Vib 1982;84(4):598–602.
[35] International Organisation for Standardization. ISO 9613-2:1996. Acoustics – Attenuation of sound during propagation outdoors – Part 2: General method of calculation.
[36] Economou P, Charalampous P. A comparison of ISO 9613–2 and advanced calculation methods using olive tree lab-terrain, an outdoor sound propagation software application: predictions versus experimental results. In: Proceedings of the Institute of Acoustics. p. 34–41.
[37] Anfosso-Lédée F. Modeling the local propagation effects of tire-road: propagation filter between CPX and CPB measurements. Proceedings of INTER NOISE, 2004. Prague, Czech Republic.
[38] International Organisation for Standardization. ISO 9613-1:1996. Acoustics – Attenuation of sound during propagation outdoors – Part 1: Calculation of the absorption of sound by the atmosphere.